FUDMA Journal of Sciences (FJS)
ISSN online: 2616-1370
ISSN print: 2645 - 2944
Vol. 7 No. 2, April, 2023, pp 188 - 198
DOI: https://doi.org/10.33003/fjs-2023-0702-1728

HEAT AND MASS TRANSFER ANALYSIS FOR THE MHD FLOW OF CASSON NANOFLUID IN THE PRESENCE OF THERMAL RADIATION

***Usman, Halima and Sulaiman, Sanusi**

Department of Mathematics, Usmanu Danfodiyo University, Sokoto, Nigeria

*Corresponding authors' email: usmanhalima6@gmail.com

ABSTRACT

This study examines how Casson nanofluid flows across a semi-infinite flat plate imbedded in a porous media while being affected by heat radiation, Soret, and pressure terms. It is considered that the surface temperature and concentration are oscillatory in nature. Water is taken into consideration as the base fluid, together with two different types of nanoparticles: copper (Cu) and titanium oxide (TiO_2). Using the regular perturbation technique, the set of ordinary differential equations is resolved. It is investigated how different flow parameters affect the Casson nanofluid in terms of velocity, temperature, concentration, and skin friction coefficient. The rate of heat transmission and the mass transfer coefficient are calculated and clearly described using graphs. It is observed that the velocity curved and the corresponding momentum boundary layer thickness decreases with increasing values of Casson parameter, this sis because Casson parameter depends on the yield stress and this stress produces a resisting force which makes the velocity curve to decrease for the increasing value of β it is also noticed that the rate of heat transfer is higher in the Cu Nanoparticles than in TiO_2 this is due to the high conductivity of the solid particles Cu than that of TiO_2 .

Keywords: MHD, Porous medium, Non-Newtonian fluid, Nanofluid, Dufour, Chemical reaction

INTRODUCTION

The theory of nanofluid was first introduced by Choi (1995) and has been a field of active research area for about two decades. Many researchers worked on heat and mass transfer on the MHD nanofluid flow. Salleh *et al*. (2010) worked on Mixed convection boundary layer flow over a horizontal circular cylinder with Newtonian heating, in their work they concluded that heat transfer from the surface is proportional to the local surface temperature. Magyari (2011) studied the homogeneous nanofluid models applied to convective heat transfer problems, in their work they investigated that the velocity slip effects of the nanoparticles \are neglected and can be reduced with the aid of elementary scaling transformations to the respective equations of the regular fluid. Mehran *et al*. (2016) have analysed the fluid flow and heat transfer analysis of a nanofluid containing motile gyro tactic micro- organisms passing a non-linear stretching vertical sheet in the presence of a non-uniform magnetic field; numerical approach and concluded that the Density number of the motile micro-organisms enhances with rise of magnetic field, Grashof number and Reynold number. Satya *et al*. (2016) have presented the heat and mass transfer on MHD nanofluid flow past vertical porous plate in a rotating system effect where they considered the effect of chemical reaction and heat source on MHD and finally figure out that the Copper nanoparticles proved to have the maximum cooling recital compared to Alumina and Titanium oxide. Prasad et al. (2018) critically analysed the heat and mass transfer analysis for the MHD flow of nanofluid with radiation absorptions. They analysed the Diffusion thermo and chemical reaction effects on the free convection heat and mass transfer flow of nanofluid over a vertical plate embedded in a porous medium in the presence of radiation absorption and heat source under fluctuating boundary conditions, they discovered that an increase in Dufour number and radiation absorption parameter leads to increase the thermal boundary layer thickness, the species concentration decreases with the increasing value of Suction parameter, Chemical reaction and Schmidt number. Baoku and Fadare (2018) studied thermo-diffusion and diffusion-thermo effects on mixed convection hydromagnetic flow in a third grade fluid over a stretching surface in a Darcy forchheimer porous medium where they found out that Soret and Dufour numbers are increasing function of the species concentration and thermal boundary thickness respectively. Fazle and Halima (2019) have examined the effect of multiple slips on the boundary layer flow of MHD nanofluid with heat and mass transfer in a Darcy porous media. In their work they considered the effect of Darcy Number and Magnetic field and found out that increasing in Darcy number and Magnetic field parameter lead to increase friction and heat transfer rate. Sehra et al. (2021) discussed the problem on convection heat mass transfer and MHD flow over a vertical plate with chemical reaction arbitrary shear stress and exponential heating. They studied Chemical Molecular Diffusivity effect and concluded that increase in Chemical reaction raise the Diffusivity of the fluid.

Non-Newtonian fluids have many applications in industries such as coolants, lubricants, heat exchangers, cosmetics and pharmaceuticals. They are attracted for scientist due to their wide applications. A theory called 'Navier stoke' is inadequate for such fluids and no single equation can exhibit the properties of all fluid. As such a number of non-Newtonian fluid models are introduced to explain the characteristics of such fluids. among them are Jeffery, Walters' B, Maxwell, Burgers and one popular and most important model called 'Casson model' this model was introduced by Casson to predict flow behaviour of pigment oil suspensions of the printing ink type (Casson 1959).

Many researchers contributed in the study of Casson fluid. Dash *et al*. (1996) have studied the Casson fluid flow in a pipe filled with a homogeneous porous medium. Their analysis can model the pathological situation of Blood flow when fatty plaques of cholesterol and artery-clogging blood clot are formed in the lumen of the coronary artery. The effect of permeability factor and yield stress of the blood on shear stress distribution, wall shear stress is analysed. Salem and Muhammad (2008) came up with the effect of hall currents and chemical reaction on hydro magnetic flow of a stretching vertical surface with internal heat generation. Their results show that the fluid velocity decrease with increasing unsteadiness parameter and temperature decrease

significantly due to unsteadiness. Swati *et al.* (2013) have presented a paper on Casson fluid over an unsteady stretching surface. In their work they analysed the effect of Casson parameter and Prandtl number and concluded that the velocity of the fluid decrease with increasing value of Casson parameter but temperature is enhanced with increasing Casson parameter. Rizwan *et al*. (2014) investigated MHD effect on Casson Nanofluid over a shrinking sheet. They considered the suction / injection effect on the wall, by applying the appropriate transformation system of non-linear partial differential equation. Farhad *et al.* (2014) have investigated closed form solutions for unsteady free convection flow of a second-grade fluid over an oscillating vertical plate. They considered the effect of Prandtl number, Grashof number, Viscos elastic parameter and phase angle Hussanan *et al.* (2014) interpreted the unsteady boundary layer flow and heat transfer of Casson fluid over an oscillating plate with Newtonian heating. They observed that velocity decrease with increase value of α and also noticed that Casson parameter does not have any influence as the fluid move away from the boundary surface. Das *et al*. (2015) discussed the Newtonian heating effect on unsteady hydro magnetic Casson fluid flow past a flat plate with heat and mass transfer. They considered the effect of Casson parameter and chemical reaction and finally discovered that the fluid velocity and temperature decrease with increasing values of Casson parameter while concentration decrease with increasing value of chemical reaction parameter and Schmidt number. Raju and Sandeep (2016) numerically analyzed dual solutions to the problem by comparing the results of Soret and Casson fluid with Newtonian fluid numerically by using mat lab bvp4c package. Sobamowo in (2018) explored on combined effects of thermal radiation and nanoparticles on free convective flow and heat transfer of Casson fluid over a vertical plate and finally investigated the effect of thermal radiation, Prandtl number, Volume fraction on the flow. Gbadeyan in (2020) illustrated the effect of variable thermal conductivity and viscosity on Casson nanofluid flow with convective heating and velocity slip. In their work they noticed that the velocity increase while both temperature and nanoparticle volume fraction decrease with increase value of variable thermal conductivity and viscosity. Mutuku and Oyen (2021) have analysed the Casson fluid of a stagnation-point flow (SPF) towards a vertical shrinking/stretching sheet. Their results show that velocity boundary layer thickness reduces with increasing value of magnetic field parameter and also the flow fluid velocity decreases with increase in Casson parameter β as well as the thermal boundary layer thickness. However, in all of the cited literatures above, none of them consider the behaviour of non-Newtonian fluid contained by a semi-infinite flat plate, as a result this study is needed.

Formulation of the problem

The flow is assumed to be in the x direction which is taken along the plate and y direction is normal to it. A uniform magnetic field of strength B_0 is taken to be acting along the y direction, it is assumed that the induced magnetic field and the external electric field due to polarization of charges are negligible and the plate and the fluid are at the same temperature T'_∞ and concentration C'_∞ in a stationary condition. The fluid is water base Casson Nanofluid containing two types of nanoparticles Cu (Copper) and TiO_2 (Titanium oxide). The nanoparticles are assumed to have a uniform shape and size also it is assumed that both the fluid and the phase nanoparticles are in thermal equilibrium state. The flow variables are function of y and t.

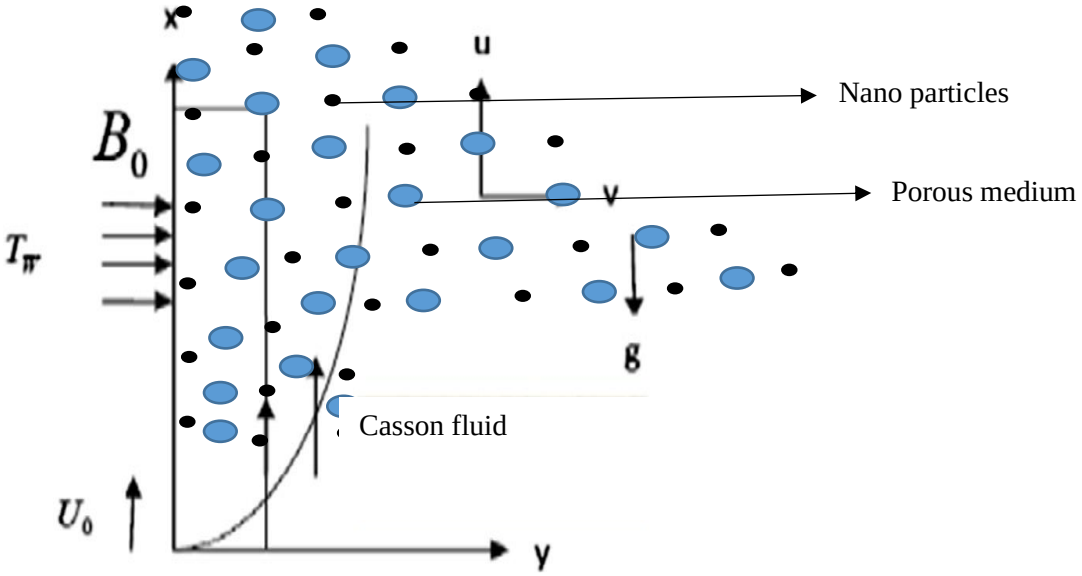

Figure 1: schematic diagram of the problem

$$\rho_{\eta f}\left(\frac{\partial u'}{\partial t'}+v'\frac{\partial u'}{\partial y'}\right)=\left(1+\frac{1}{\beta}\right)\mu_{\eta f}\frac{\partial^2 u'}{\partial y'^2}+(\rho\beta)_{\eta f}g(T'-T'_\infty)-\frac{\mu_{\eta f}u'}{k'}-\sigma {B_0}^2 u' \quad (1)$$

$$\left(\frac{\partial T'}{\partial t'}+v'\frac{\partial T'}{\partial y'}\right)=\alpha_{\eta f}\frac{\partial^2 T'}{\partial y'^2}-\frac{Q'}{(\rho C_\rho)_{\eta f}}(T'-T'_\infty)+Q'_l(C'-C'_\infty)+\frac{D_m k_T}{C_s(\rho C_\rho)}\frac{\partial^2 C'}{\partial y'^2} \quad (2)$$

$$\frac{\partial C'}{\partial t'}+v'\frac{\partial C'}{\partial y'}=D_B\frac{\partial^2 C'}{\partial y'^2}-k_l(C'-C'_\infty) \quad (3)$$

Boundary conditions for the problem are given by

$$t' < 0, u'(y', t') = 0, T' = T'_{\infty}, C' = C'_{\infty}$$

$$t' \geq 0, u'(y', t') = U_0, T' = T'_w + (T' - T'_{\infty})\varepsilon e^{iw't'}, C' = C'_w + (C'_w - C'_{\infty})\varepsilon e^{iw't'}, aty' = 0 \quad (4)$$

$$u'(y', t') = 0, T' = T'_{\infty}, C' = C'_{\infty}, aty' \to \infty$$

Dimensionless quantities

$$u = \frac{u'}{U_0}, y = \frac{U_0 y'}{v_f}, t = \frac{U_0 t'}{v_f},$$
$$\theta = \frac{(T' - T'_{\infty})}{(T'_w - T'_{\infty})}, S = \frac{V_0}{U_0}, M = \frac{\sigma {B_0}^2 v_f}{\rho_f {U_0}^2},$$
$$Du = \frac{D_m K_T (C'_w - C'_{\infty})}{k_f C_s (T' - T'_{\infty})}, Q_L = \frac{Q'_l (C'_w - C'_{\infty})}{{U_0}^2 (T'_w - T'_{\infty})}$$
$$\psi = \frac{(C' - C'_{\infty})}{(C'_w - C'_{\infty})}, Gr = \frac{(\rho\beta)_f g v_f (T'_w - T'_{\infty})}{\rho_f {U_0}^2}$$
$$Q = \frac{Q' {v_f}^2}{K_f {U_0}^2}, Pr = \frac{v_f}{\alpha_f}, K = \frac{k' \rho_f {U_0}^2}{{v_f}^2}$$
$$Kr = \frac{K_l {v_f}^2}{K_f {U_0}^2}, Sc = \frac{v_f}{D_B} \quad (5)$$

The following non dimensional differential equations are obtained

$$A\left(\frac{\partial u}{\partial t} - S\frac{\partial u}{\partial y}\right) = D\left(1 + \frac{1}{\beta}\right)\frac{\partial^2 u}{\partial y^2} + BGr\theta - \left(M + \frac{1}{K}\right)u \quad (6)$$

$$C\left(\frac{\partial \theta}{\partial t} - S\frac{\partial \theta}{\partial y} - Q_L\psi\right) = \frac{1}{\mathrm{Pr}}\left(E\frac{\partial^2 \theta}{\partial y^2} - Q\theta\right) + \frac{Du}{\mathrm{Pr}}\frac{\partial^2 \psi}{\partial y^2} \quad (7)$$

$$\frac{\partial \psi}{\partial t} - S\frac{\partial \psi}{\partial y} = \frac{1}{Sc}\frac{\partial^2 \psi}{\partial y^2} - Kr\psi \quad (8)$$

METHOD OF SOLUTION

The above PDE is resolved by the well-known regular perturbation method. The unsteady flow is superimposed on the mean steady flow, so that in the neighbourhood of the plate, the expressions for velocity, temperature, and concentration are assumed as.

$$\psi(y, t) = \psi_0 + \varepsilon\psi_1 e^{t\omega t} \quad (9)$$

$$u(y, t) = u_0 + \varepsilon u_1 e^{i\omega t} \quad (10)$$

$$\theta(y, t) = \theta_0 + \varepsilon\theta_1 e^{i\omega t} \quad (11)$$

Where $\varepsilon << 1$

$$u(y, t) = (B_5 e^{-m5y} + B_3 e^{-m3y} + B_4 e^{-m1y}) + \varepsilon(B_8 e^{-m6y} + B_6 e^{-m4y} + B_7 e^{-m2y})e^{i\omega t} \quad (12)$$

$$\theta(y, t) = (B_1 e^{-m3y} + A_1 e^{-m1y}) + \varepsilon(B_2 e^{-m4y} + A_2 e^{-m2y})e^{i\omega t} \quad (13)$$

$$\psi(y, t) = (e^{-m1y}) + \varepsilon(e^{-m2y})e^{i\omega t} \quad (14)$$

$$Nu = -\left(\frac{\partial \theta}{\partial t}\right)_{y=0} = (B_1 m_3 + A_1 m_1) + \varepsilon(B_2 m_4 + A_2 m_2)e^{i\omega t} \quad (15)$$

$$Sh = -\left(\frac{\partial \psi}{\partial t}\right)_{y=0} = m_1 + \varepsilon m_2 e^{i\omega t} \quad (16)$$

$$\tau = \left(\frac{\partial u}{\partial t}\right)_{y=0} = (-B_5 m_5 - B_3 m_3 - B_4 m_1) + \varepsilon(-B_8 m_6 - B_6 m_4 - B_7 m_2)e^{i\omega t} \quad (17)$$

RESULTS AND DISCUSSIONS

The values of the parameters ($Pr = 0.71, \omega = 1, t = 1, \varepsilon = 0.02$, $Du = 2$, $Q_L = 2Q_L = 2$, $\beta = 2\beta = 2$, $K = 5$, $Gr = 2Gr = 2$, $Q = 2$, $S = 0.1$, $Kr = 0.1$, $Sc = 0.6$, $M = 0.6$) are kept unchanged throughout the study unless otherwise stated.

Figure (1a) and (1b) demonstrates the velocity profiles, it is observed that, velocity curve and the corresponding momentum boundary layer thickness decreases with increasing values of Casson parameter, this is because Casson parameter depends on the yield stress and this stress produces a resisting force which makes the velocity curve to decrease for the increasing value of β.

Figure (2a), (2b) and (7a),(7b) illustrates the effects of DuFour for velocity and temperature respectively for both the Cu and TiO_2 nanoparticles. It is noticed that both velocity and temperature enhance the thermal boundary layer thickness. Thermal boundary layer thickness is high. Physically the DuFour term measures the contribution of concentration gradient to thermal energy flux in the flow domain, it has a vital role in enhancing the flow velocity and the ability to increase the thermal energy in the boundary layer, that is why the temperature profile increases with the increase of Du.

Figure (3a) ,(3b) and (6a), (6b) shows the effects of radiation absorption (Q_L) on velocity and temperature, it is clearly noticed that both velocity and temperature increase with increasing value of radiation absorption(Q_L)

Figure (4a) and (4b) demonstrates the effects of Magnetic parameter (M) on velocity profile. It clearly shows that the velocity profile drops when magnetic parameter increases. This is because when magnetic parameter increase, the Lorentz force also will increase and caused to oppose the fluid motion.

Figure (5a) and (5b) shows the effects of suction parameter (S) on the velocity profile. It is seen that the velocity of the fluid across the boundary layer is decreasing by increasing the value of suction parameter for both the pure and Casson Nano fluid.

Figure 8: demonstrate the effect of suction parameter (S) and Schmidt number (Sc) on concentration profile. It is well noticed that increases in suction decrease the boundary layer of the concentration profile. it is also noticed that increase in Schmidt number corresponds to a weaker solute diffusivity which allows a shallower penetration of solute effect. As a result, the concentration decreases with increase in Sc.

Figure 9: shows the effect of chemical reaction (Kr) on concentration profile. Its observed that increase in chemical reaction parameter decreases the concentration profile. The rationale is that as chemical reactions increases, the quantity of solute molecules undergoing them grows, this causes concentration to drop, which in turn reduces the like hood of destructive chemical reaction.

Figure 10 (a) and (b), 11 (a) and (b) and figure 12 shows that the skin friction decrease with increasing value of Casson parameter (β) while increase with increasing value of Radiation parameter (QL) and Dufour (Du).

Figure 13 (a) and (b) illustrates the graph of Nusselt number and it is well noted that the Nusselt number decreases with increasing value of the radiation absorption parameter (QL), Dufour (Du) and Suction (S).

Figure 14 (a), (b) and 15 shows the graph of Sherwood number and it is noticed that the Sherwood number decreases with increasing value of Schmidt number (Sc) chemical reaction (Kr) and Suction parameter (S) respectively.

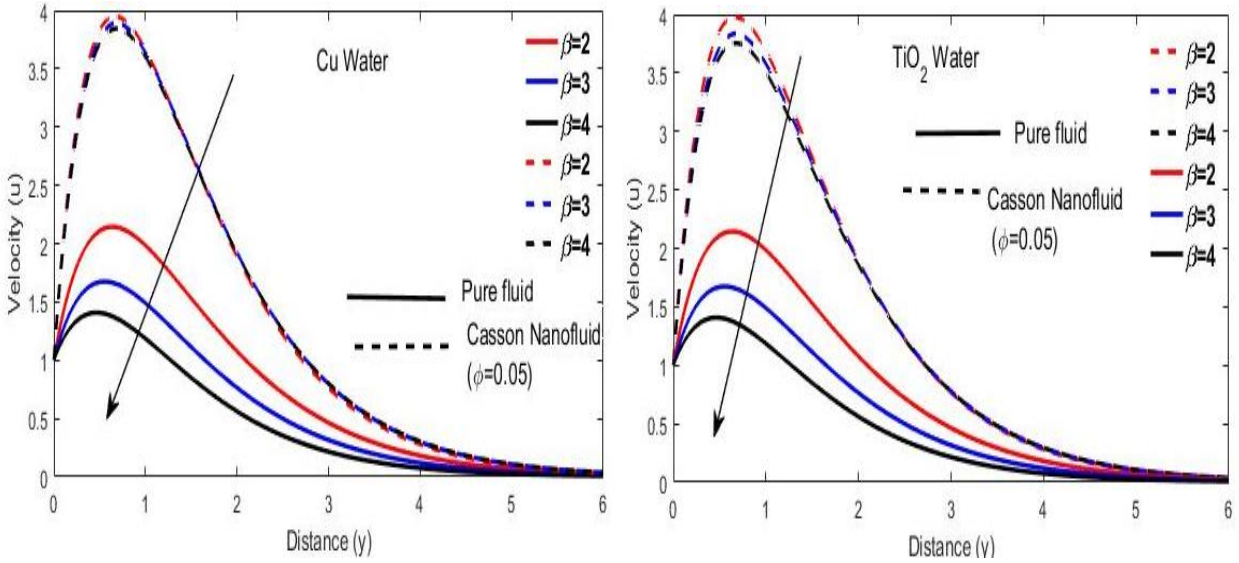

Figure 1: (a) and (b) Velocity profiles showing the effects of Casson parameter (β).

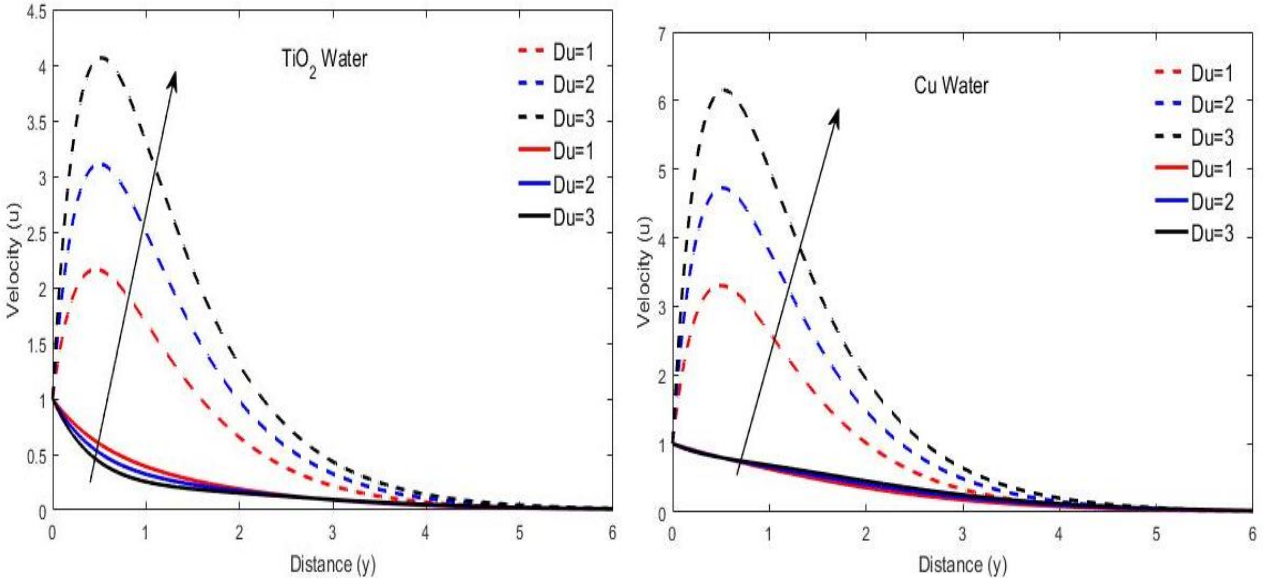

Figure 2: (a) and (b) Velocity profiles showing the effects of Dufour (Du)

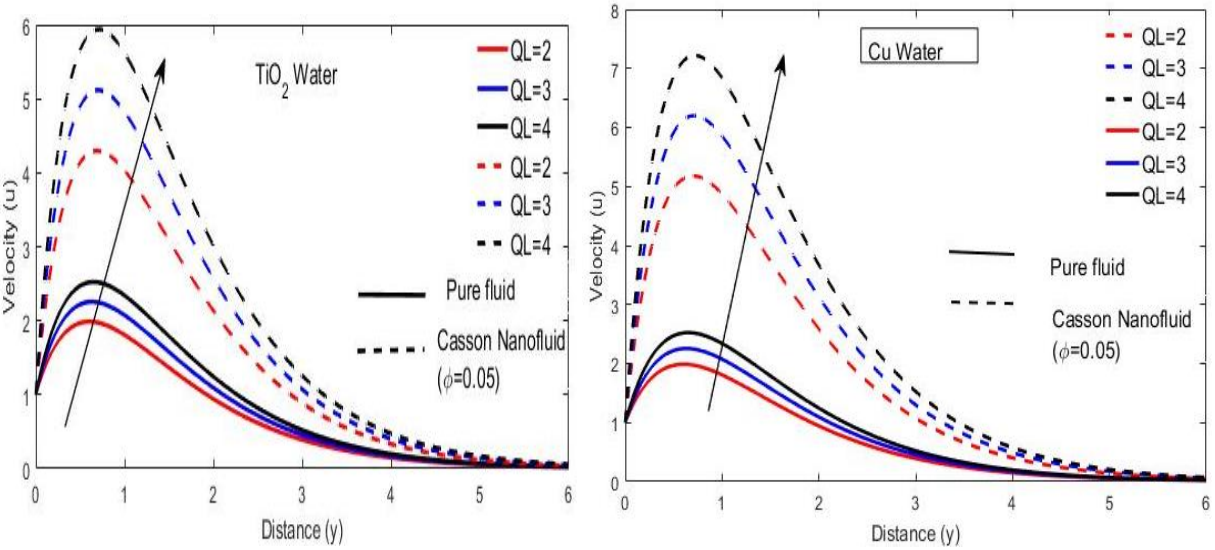

Figure 3: (a) and (b) Velocity profiles showing the effects of Radiation absorption parameter (QL).

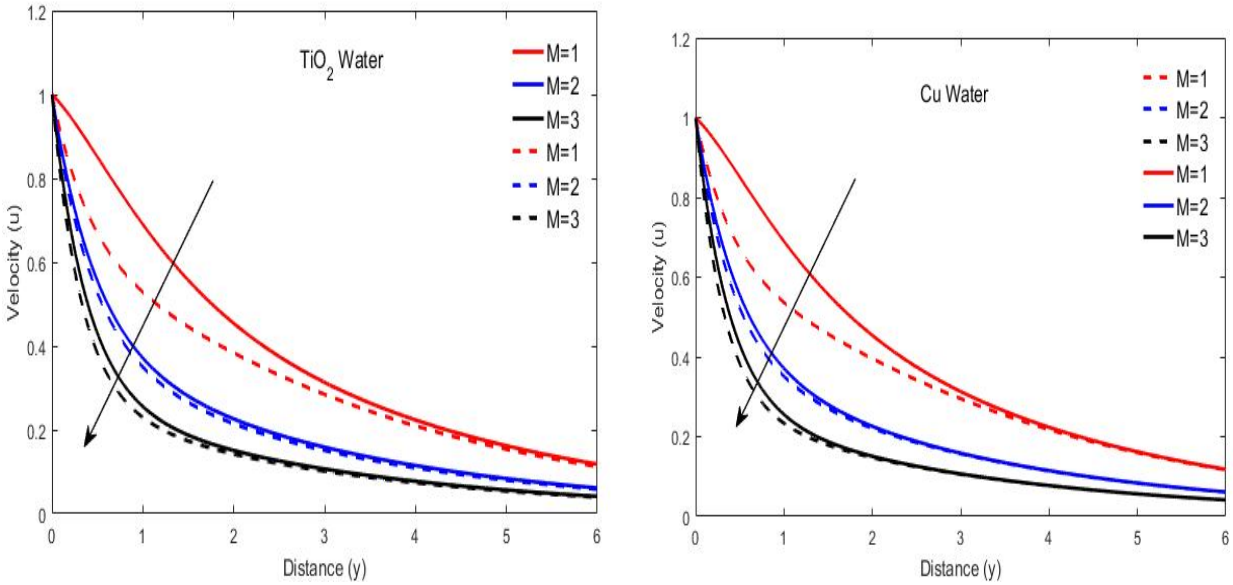

Figure 4: (a) and (b) is Velocity profile showing the effects of Magnetic field (QL).

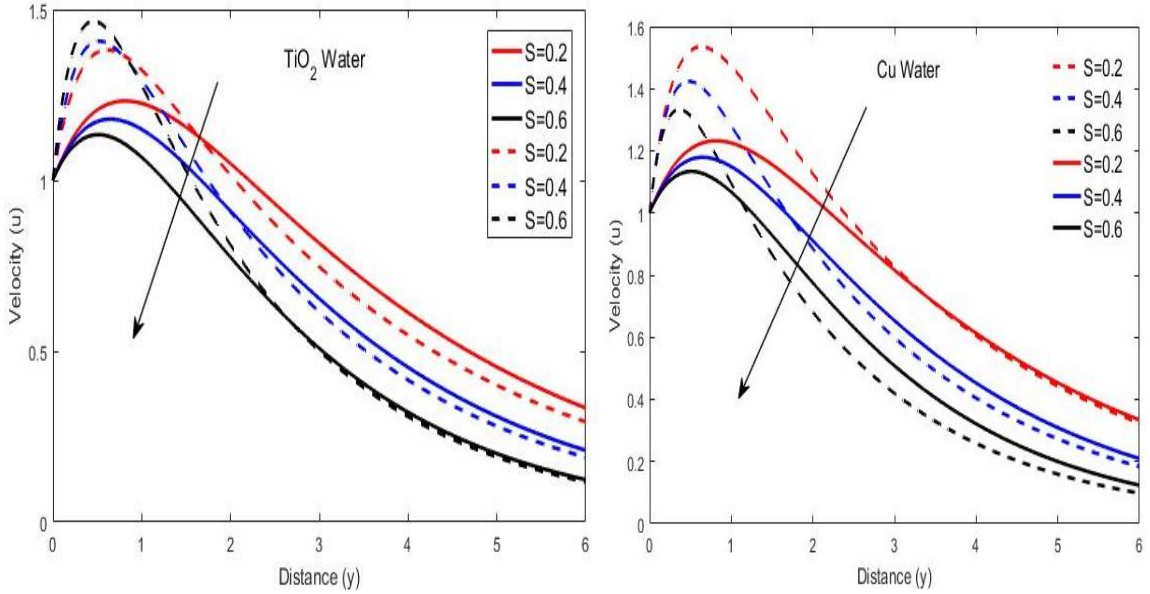

Figure 5: (a) and (b) Velocity profiles showing the effects of Suction (S).

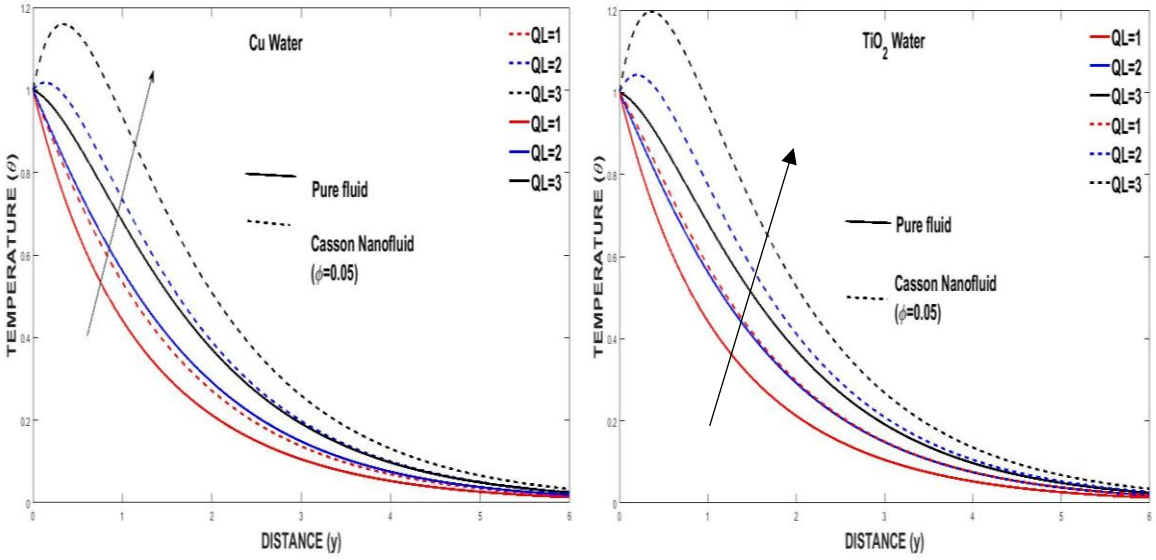

Figure 6: (a) and (b) Temperature profiles showing the effects of radiation absorption (QL)

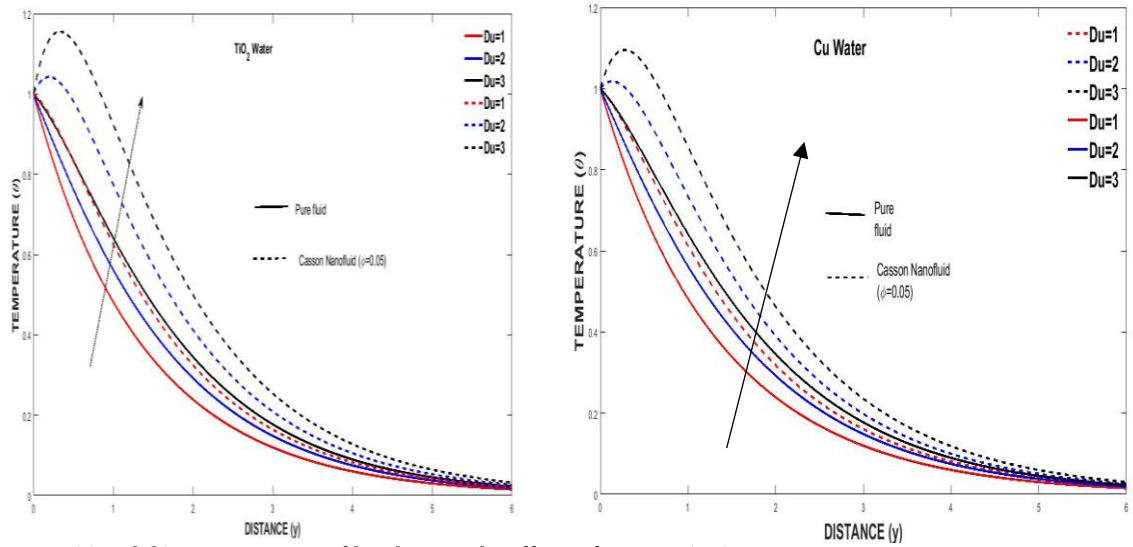

Figure 7: (a) and (b) Temperature profiles showing the effects of DuFour (Du).

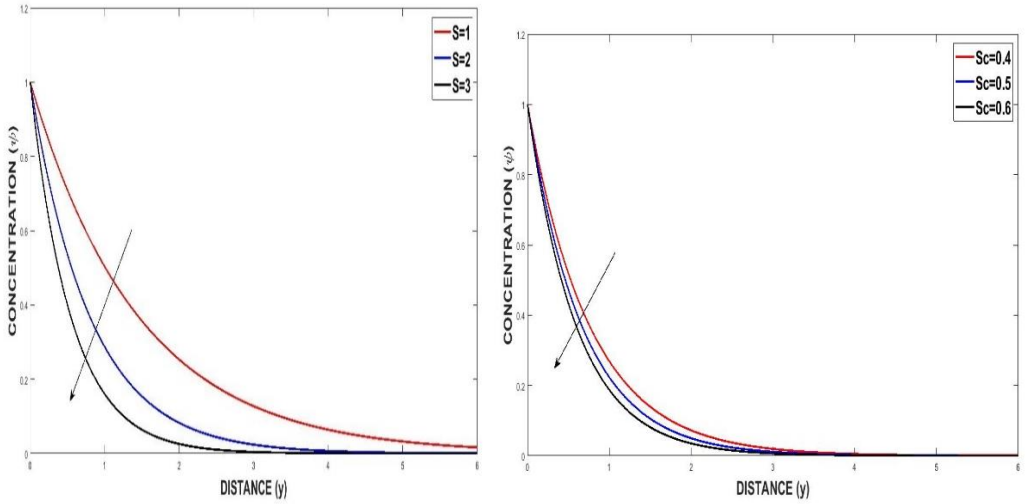

Figure 8: (a) and (b) Concentration profile showing the effects of suction (S) and Shmidt number (Sc) respectively.

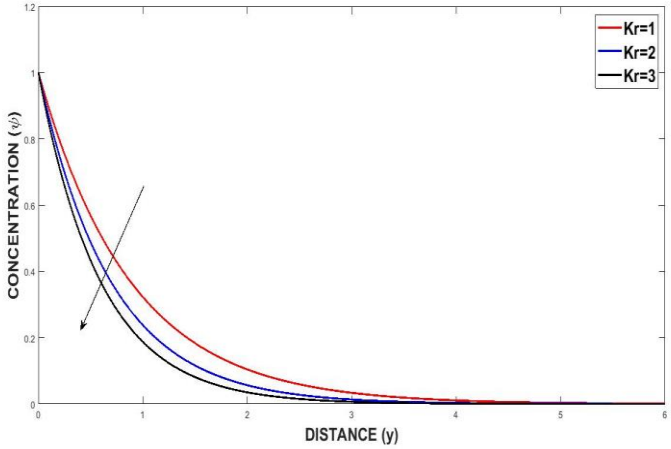

Figure 9: Concentration profile showing the effect of Chemical reaction (Sc).

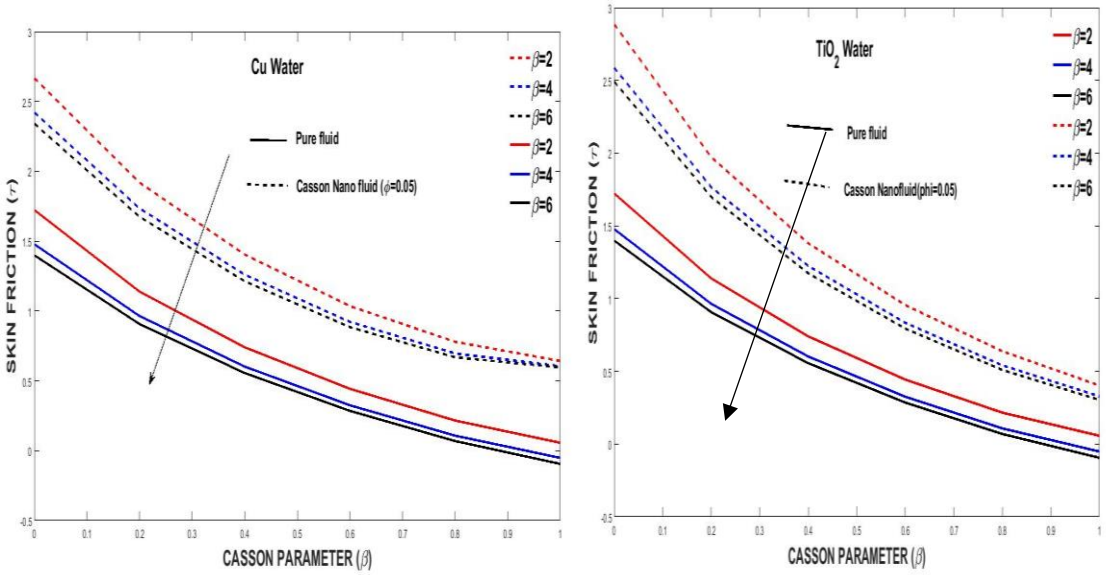

Figure 10: (a) and (b) Skin friction profile showing the effects Casson parameter (β).

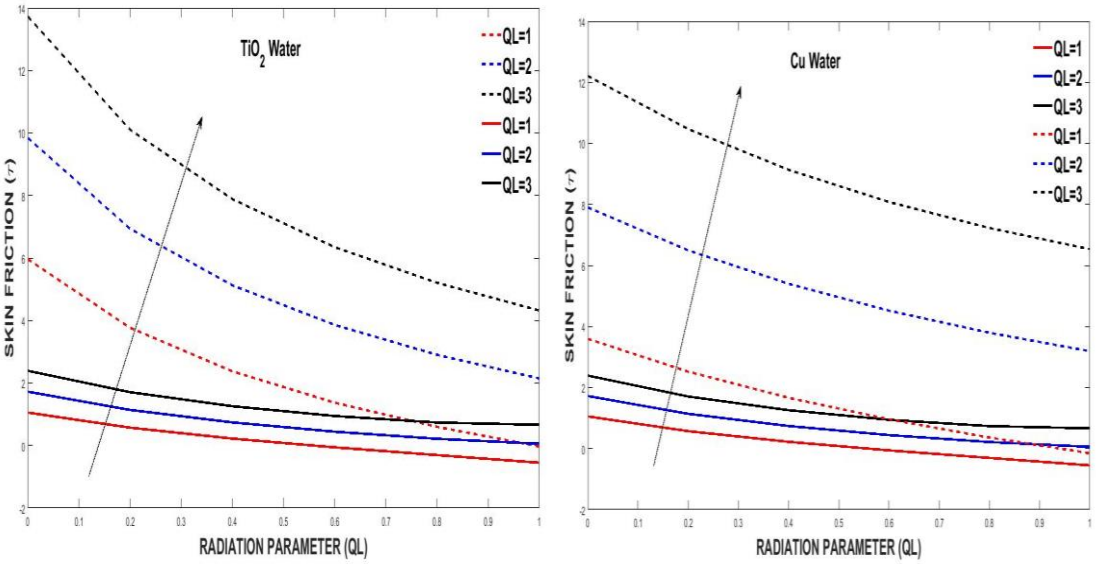

Figure 11: (a) and (b) Skin friction profile showing the effect of Radiation absorption parameter (QL).

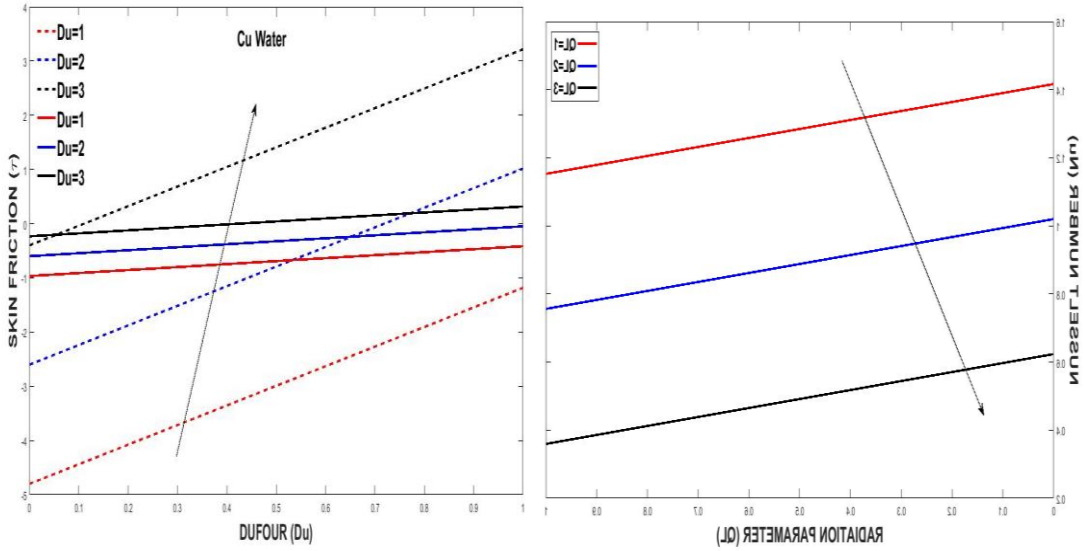

Figure 12: (a) and (b) Skin friction profile showing the effect of Dufour (Du) and radiation parameter (QL) on Nusselt number.

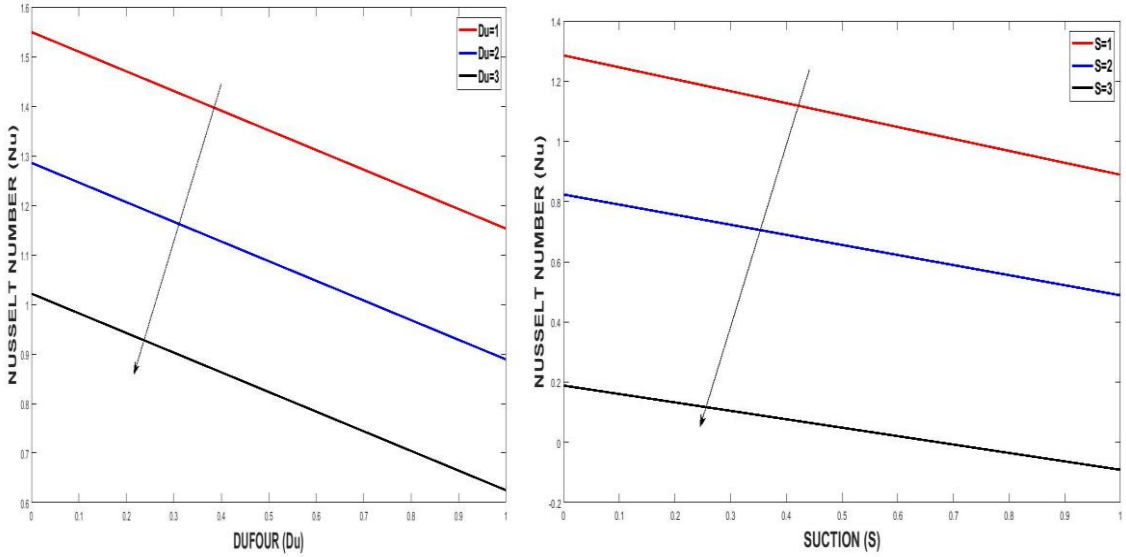

Figure 13: Effect of Dufour (Du) and Suction (S) on Nusselt number.

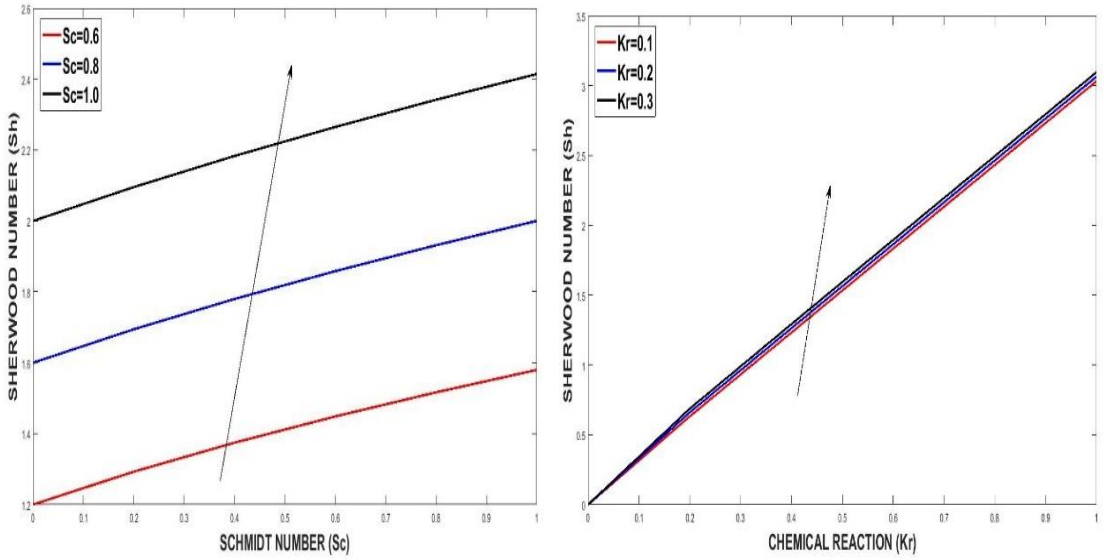

Figure 14: Effect of Schmidt number (Sc) and chemical reaction (Kr) on Sherwood number.

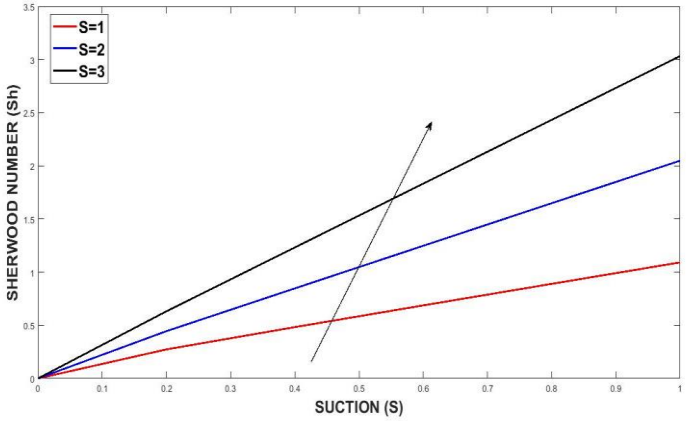

Figure 15: Effect of Suction (S) on Sherwood number (Sh) with Kr=0.1 and Sc=0.6

CONCLUSION

In the present study, we have theoretically studied the effects of the metallic nanoparticles on the unsteady MHD free convective flow of incompressible Casson Nanofluid past a moving infinite vertical porous plate. The set of governing equation are solved analytically by using perturbation technique. The effects of various fluid flow parameters on velocity, temperature, concentration, skin friction, Nusselt number and Sherwood number are derived and discussed through graphs. The following conclusion are made from the present investigation:

i. Velocity decreases with the increase in the value of Casson parameter (β), Magnetic field parameter (M) and Suction parameter (S) while it increases with the increase in the value of Dufour (Du) and Radiation absorption parameter (QL).
ii. Temperature increases with the increase in the value of Dufour (Du) and radiation absorption parameter (QL).
iii. Concentration profile decrease with increase in the value of Schmidt number (Sc), chemical reaction (Kr) and suction parameter (S).
iv. skin friction profile reduces as Casson parameter rise while increases as radiation absorption (QL) and Dufour (Du) rise.
v. Nusselt number profile decreases with increase in the value of Dufour (Du), radiation absorption (QL) and Suction parameter (S).
vi. Sherwood number profile increase with increase in the value of chemical reaction (Kr), Schmidt number (Sc) and Suction parameter (S).

$APPENDIX$

$$A = \left((1-\phi) + \phi\left(\frac{\rho_s}{\rho_f}\right)\right), B = \left((1-\phi) + \phi\left(\frac{(\rho\beta)_s}{(\rho\beta)_f}\right)\right)$$

$$C = \left((1-\phi) + \phi\left(\frac{(\rho C_\rho)_s}{(\rho C\rho)_f}\right)\right)$$

$$E = \frac{\left((1+2\phi)+(2-2\phi)\left(\frac{k_f}{k_s}\right)\right)}{\left((1-2\phi)+(2+2\phi)\left(\frac{k_f}{k_s}\right)\right)}, D = \frac{1}{(1-\phi)^{2.5}}$$

$$A_1 = \left(\frac{{m_1}^2 Du + Pr\, Q_L\, C}{E{m_1}^2 - Pr\, C\, Sm_1 - Q}\right)$$

$$A_2 = -\left(\frac{{m_2}^2 Du + Pr\, Q_L\, C}{E{m_2}^2 - Pr\, C\, Sm_2 - (Q + i\omega\, Pr\, C)}\right)$$

$$B_1 = (1 - A_1), B_2 = (1 - A_2)$$

$$B_3 = \frac{-BB_1Gr}{D\left(1+\frac{1}{\beta}\right){m_3}^2 - ASm_3 - \left(m+\frac{1}{k}\right)}$$

$$B_4 = \frac{-BA_1Gr}{D\left(1+\frac{1}{\beta}\right){m_1}^2 - ASm_1 - \left(m+\frac{1}{k}\right)}$$

$$B5 = 1 - B_3 - B_4$$

$$B_6 = \frac{-BB_2Gr}{D\left(1+\frac{1}{\beta}\right){m_4}^2 - ASm_4 - \left((m+\frac{1}{k}) + Ai\omega\right)}$$

$$B_7 = \frac{-BA_2Gr}{D\left(1+\frac{1}{\beta}\right){m_2}^2 - ASm_2 - \left((m+\frac{1}{k}) + Ai\omega\right)}$$

$$B_8 = 1 - B_6 - B_7$$

$$m_1 = \frac{SSc + \sqrt{(SSc)^2 + 4KrSc}}{2}$$

$$m_2 = \frac{SSc + \sqrt{(SSc)^2 + 4Sc(i\omega + Kr)}}{2}$$

$$m_3 = \frac{Pr\, C\, S + \sqrt{(Pr\, C\, s)^2 + 4EQ}}{2E}$$

$$m_4 = \frac{Pr\, C\, S + \sqrt{(Pr\, C\, S)^2 + 4E(Q + i\omega Pr())}}{2E}$$

$$m_5 = \frac{AS + \sqrt{(AS)^2 + 4D\left(1+\frac{1}{\beta}\right)\left(m+\frac{1}{K}\right)}}{2D\left(1+\frac{1}{\beta}\right)}$$

$$m_6 = \frac{AS + \sqrt{(AS)^2 + 4D\left(1+\frac{1}{\beta}\right)\left((m+\frac{1}{K}) + Ai\omega\right)}}{2D\left(1+\frac{1}{\beta}\right)}$$

REFERENCES

Baoku, I., & Fadare, S.A. (2018). Thermo-diffusion and diffusion -thermo effects on mixed convection hydromagnetic flow in a third-grade fluid over a stretching surface in a Darcy forchheimer porous medium. *FUDMA journal of sciences*, 2(1), 23-42.

Casson, N. (1959). flow equation for pigment oil suspensions of the printing ink type. *Rheology of disperse systems*, 84:2.

Choi, S.U., Eastman, J.A. (1995). *Enhancing thermal conductivity of fluids with nanoparticles*. (No. ANL/MSD/CP-84938: CONF-951135-29.

Das, M., Mahato, R., & Nandkeolyar, R. (2015). Newtonian heating effect on unsteady hydro magnetic Casson fluid flow past a flat plate with heat and mass transfer. *Alexandria engineering journal*, 54(4), 871-879.

Dash, R.K., Mehta, K.N., & Jayaraman, G. (1996). The flow characteristics of a Casson fluid in a tube filled with a homogeneous porous medium. *International journal of engineering science*, 34(10), 1145-1156.

Gbadeyan, J.A., Titiloye, E.O., & Adeosun, A.T. (2020). Effect of variable thermal conductivity and viscosity on Casson nanoflui9d flow with convective heating and velocity slip. *Heliyon*, 6(1), e03076.

M. Mehryan, S.A., Moradi Kashkooli, F., Soltani, M., & Raahemifar, K. (2016). Fluid flow and heat transfer analysis of a nanofluid containing motile gyrotactic micro-organisms passing a nonlinear stretching vertical sheet in the presence of a non-uniform magnetic field; numerical approach. *PLos One*, 11(6), e0157598.

Mabood, F., & Usman, H. (2019). Multiple slip effects on MHD thermo-solutal flow in porous media saturated by nanofluid. *Mathematical modelling of engineering problems*, 6(4), 502-510.

Magyari, E. (2011). Comment on the homogeneous nanofluid models applied to convective hear transfer problems. *Acta mechanica*, 222(3-4), 381-385.

Mutuku, W.N., & Oyen, A.O. (2021). Casson fluid of a stagnation-point flow (SPF) towards a vertical shrinking/stretching sheet. *FUDMA journal of sciences*, 5(1), 16-26.

Prasad, P.D., Kumar, R.K., & Varma, S.V.K. (2018) heat and mass transfer analysis for the MHD flow of nanofluid with

radiation absorption. Ain Shams Engineering Journal, 9(4), 801-813.

Raju, C.S.K., Sandeep, N., Sugunamma, V., Babu, M.J., & Reddy, J.R. (2016). Heat and mass transfer in magnetohydrodynamic Casson fluid over an exponentially permeable stretching surface. *Engineering Science and Technology, an International Journal*, 19(1), 45-52.

Salem, A.M., & Abd El-Aziz, M. (2008). Effect of Hall currents and chemical reaction on hydromagnetic flow of a stretching vertical surface with internal heat generation/absorption. *Applied Mathematical Modelling*, 32(7), 1236-1254.

Salleh, M.Z., Nazar, R., & Pop, I. (2010). Mixed convection boundary layer flow over a horizontal circular cylinder with Newtonian heating. *Heat and mass transfer*, 46, 1411-1418.

Satya Narayana, P.V., & Venkateswarlu, B. (2016). Heat and mass transfer on MHD nanofluid flow past a vertical porous plate in a rotating system. *Frontiers in heat and mass transfer (FHMT)*, 7(1).

Sobamowo, M.G. (2018). Combined effects of thermal radiation and nanoparticles on free convection flow and heat transfer of Casson fluid over a vertical plate. *International Journal of Chemical Engineering*, 2018.